energies

MDPI

Article

Analysis of the Channel Influence to Power Line Communications Based on ITU-T G.9904 (PRIME)

Asier Llano [1,*], Itziar Angulo [2,†], Pablo Angueira [2,†], Txetxu Arzuaga [1,†] and David de la Vega [2,†]

Received: 31 August 2015; Accepted: 4 January 2016; Published: 12 January 2016
Academic Editor: Thorsten Staake

1 Engineering Department, Distribution Automation Solutions (DAS), ZIV, Parque Tecnológico 210, 48170 Zamudio, Spain; txetxu.arzuaga@cgglobal.com
2 Department of Communications Engineering, University of the Basque Country (UPV/EHU), Alameda Urquijo s/n, 48013 Bilbao, Spain; itziar.angulo@ehu.es (I.A.); pablo.angueira@ehu.es (P.A.); david.delavega@ehu.es (D.V.)
* Correspondence: asier.llano@cgglobal.com; Tel.: +34-657-707-735
† These authors contributed equally to this work.

Abstract: ITU-T G.9904 standard, also known as PoweRline Intelligent Metering Evolution (PRIME), is a Power Line Communications standard for advanced metering, grid control and asset monitoring defined by the International Telecommunication Union (ITU). In this paper, an analysis about how different characteristics of the communication channel and types of noise might affect the system performance is carried out. This study is based on simulations of the PRIME physical layer using different channel characteristics and transmission parameters. The conclusions obtained are very valuable for better understanding the behavior of the ITU-T G.9904 (PRIME) standard in the field, allowing future improvements in deployment strategies and equipment design.

Keywords: electromagnetic noise; ITU-T G.9904; power line communications; PRIME; smart grid; smart metering

1. Introduction

Low Voltage (LV) Power Line Communications (PLC) are a key technology for electric distribution automatization, also known as Smart Grids. The most complicated and expensive part of the electric distribution automation is the low voltage automation, due to the number of points to communicate and their dynamic nature.

For this challenge, Low Voltage PLC systems have the advantage of not requiring a specific communication medium deployment, providing an owned network infrastructure with simple installation.

The electric line, as a communication channel, has a very variable impedance and transference function. The noise of the channel is also very particular, due to its nature. This noise is originated by the devices connected to the network as loads or generators, and their characteristics strongly depend on each noise source device particular design. The channel is variable in time, due to consumer habits, generation cycles and technology changes, among other factors. It is also variable in space, between rural and urban areas, and between different countries/regions, due to differences in energy consumption habits, lines distribution and consumer/generator technologies.

On one hand, it is important to analyze the characteristics of the PLC propagation channel. Some studies have been carried out to analyze this transmission medium characteristics, such as impedance, attenuation, phase shift, noise classification and characterization. As the PLC propagation channel characteristics depend on the particularities of the consumption, generation and distribution of energy, these studies usually perform field measurements in real lines or laboratory measurements

with real noise sources in order to extract relevant statistic information. References [1–3] present studies of most characteristics of this propagation channel. More recent articles focus on particular channel effects and/or noise models. As an example, reference [4] focuses on non-synchronous impulsive noise modeling, while [5] is centered on narrowband noise modeling.

On the other hand, the analysis on how the different characteristics of the propagation channel affect the PLC technologies complement the noise studies. Several references focus on these effects for generic PLC communication systems, like reference [6], which analyzes the influence of the phase distortion on correlation based PLC systems; reference [7], which studies the convolutional encoding performance over channels with noise modeled using a partitioned Markov chain; or reference [8] which investigates the impact of asynchronous impulsive noise on Orthogonal Frequency Division Multiplexing (OFDM) and Offset Quadrature Amplitude Modulation (OQAM). Some other studies analyze the influence of the channel distortions on G3 and PoweRline Intelligent Metering Evolution (PRIME) standard technologies. Reference [9] is focused on the performance of PRIME technology under impulsive noise environments. In [10], the performance of PRIME and G3 systems under white noise, periodic impulsive noise in the time-domain, and narrowband co-channel interference is analyzed. In [11], the physical layers of G3 and PRIME are compared to each other, by theoretical analysis as well as simulation results.

There are several recent articles that reveal the need for additional research on the effects of the channel disturbances. Reference [12] (p. 909) mentions this need: "There is now a general acceptance of the need for research to understand origin, spread and consequences of emission in this frequency range". Reference [13] (p. 114) states: "There is a serious interest from the international standard-setting community in knowledge in the frequency range 2–150 kHz. At the same time research is ongoing at a number of locations, but the knowledge about this frequency range remains limited." Report [14] (p. 72) requires further investigation: "Further investigations on EMI in the frequency range 2–150 kHz appear as being of interest."

The need for further investigations and the scarcity of studies in the frequency range where PRIME is used lead to a research line in which many channel characteristics are analyzed and their effects on standard PLC technologies are evaluated. This research has a broader scope than other studies found in the literature, not being limited to a single type of channel distortion as compared to [9]. On the contrary, it encloses simultaneously different channel responses and different noise patterns, which are analyzed, compared and related in the same study environment, and their influence on LV PLC performance is assessed. Moreover, unlike previous research about periodic impulsive noise [9,10], the parameters that define the characteristics of the noise are configurable and this way, the obtained results can be applied to a wider casuistic. Finally, the simulations are based on a realistic fully PRIME compliant software (SW) platform that includes the same physical layer available in commercial hardware (HW) devices, which gives the study a point of view closer to practical implementations as compared to [11].

2. Scope of the Paper

This article is focused on analyzing how different parameters of the channel and types of noise affect one of the standard PLC technologies deployed in Europe: ITU-T G.9904 (PRIME v1.3.6) defined by the Internation Telecommunication Union (ITU) in Reference [15]. This study is based on simulations of the PRIME physical (PHY) layer using different channel characteristics and different transmission parameters:

- Channel configurable parameters.
  - Channel response function, usually defined by its response in module and phase (described in Section 4.2).
  - Noise model (described in Section 4.3).
  - Signal-to-Noise Ratio (SNR).

- Transmission configurable parameters.
  - Modulation scheme: Differential Binary Phase-Shift Keying (DBPSK), Differential Quadrature Phase-Shift Keying (DQPSK) and Differential 8 Phase-Shift Keying (D8PSK) with and without convolutional encoding.
  - Packet Service Data Unit (PSDU) length.

The purpose of each simulation is to identify the PRIME behavior under individual channel effects. The understanding of the technology based on the conclusions of this article will be used to:

- Better understand individual issues, giving the information needed to identify and compare these individual channel effects on field deployments in order to evaluate how they might affect the network performance.
- Guide deployment strategies.
- Evaluate current PLC technologies to enhance their features in future developments.
- Obtain values of parameters to compare PLC technologies and choose the one best suited to a particular environment or application.

Although the PLC propagation channel in the field is variable in time, in most situations, it is useful to consider it quasi-stationary, or stable enough along one single PHY Packet Data Unit (PPDU). Additionally, despite the fact that the real PLC propagation channel is more complex, it is also useful to consider it as a combination of several individual channel effects. In most situations, one (or a few) of these effects will be the determining factors that impose the Frame Error Rate (FER), and their nature and results could be compared with the results provided in this paper.

3. Brief Description of ITU-T G.9904 (PRIME) Physical Layer

The PLC communication system described in ITU-T G.9904 [15] (also known as PRIME) is based on an Orthogonal Frequency Division Multiplexing (OFDM) physical layer.

The block diagrams of the physical layer transmitter and receiver form a classical OFDM chain, as depicted in Figures 1 and 2.

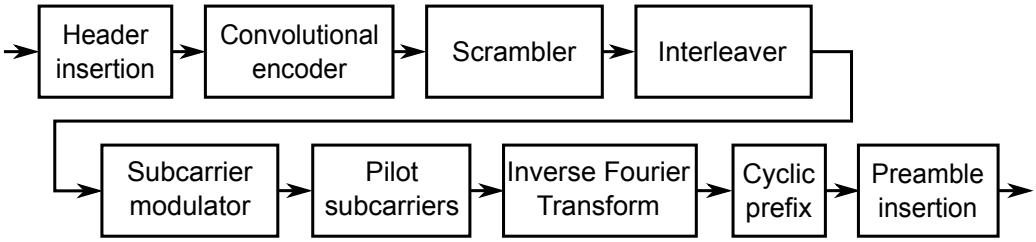

Figure 1. PRIME PHY layer transmission block diagram.

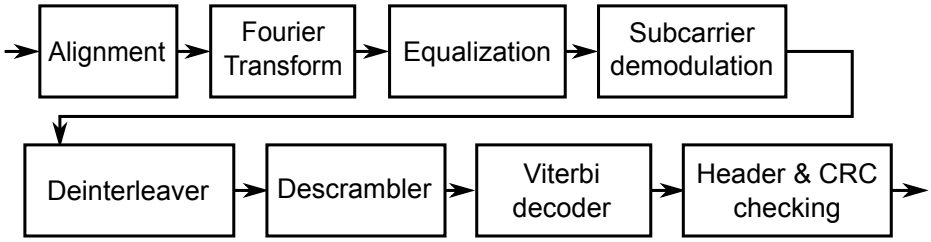

Figure 2. PRIME PHY layer reception block diagram.

The most important parameters of the OFDM modulation are summarized in Table 1. For more detailed information about the ITU-T G.9904 standard, refer to the specifications in [15–17].

Table 1. ITU-T G.9904 (PRIME) physical parameters.

Parameter	Value
Frequency band	41.9–88.9 kHz
Number of subcarriers	97
Intercarrier spacing	488.28 Hz
OFDM symbol length	2.24 ms
Cyclic prefix length	192 μs
Interleaver type	Block interleaver
Interleaver size	1 OFDM symbol
Encoder rate	1/2
Subcarrier modulation	DBPSK: Differential Binary Phase-Shift Keying DQPSK: Differential Quadrature Phase-Shift Keying D8PSK: Differential 8 Phase-Shift Keying
Preamble waveform	Single chirp from 41.9–88.9 kHz in 2.048 ms

4. Workbench Description and Test Conditions

4.1. Implementation of the ITU-T G.9904 (PRIME) Layer Used for the Simulation

For the above mentioned purposes, a complete ITU-T G.9904 (PRIME) device, which works in real HW and inside a Personal Computer (PC), has been carried out. It is the same physical layer included in the PRIME devices from ZIV (as shown in [18]).

The implementation of this physical layer has been performed following PRIME specifications as in [15–17]. It has been certified by independent laboratories (Tecnalia, ITE, Kema) following the Certification Test Book of the PRIME Alliance [19]. Several million of PRIME meters are currently installed on field with this implementation. Regarding the applicability of the results presented in this paper, tests carried out by the PRIME Alliance Members assure that PRIME certified products have similar performance and as such, the obtained results will also apply to other HW implementations.

The implementation of the PRIME physical layer has been done mostly in C but optimized in assembler for some platforms. The simulation environment is executed with the same modem in a PC environment in which PLC modems communicate to each other using Inter Process Communication (IPC) sockets. The propagation channel simulator is performed in an additional computer process which takes the representation of the analog signal, processes it and interchanges it with the modems.

Some control measurements have been performed to check that the provided simulation data match with the results obtained with real HW devices in laboratory conditions. The tests have been performed for control points of $FER = 0.1$ and $FER = 0.01$ for the Additive White Gaussian Noise (AWGN) noise, synchronous impulsive noise and frequency selective channel for the same modulation schemes evaluated in Section 6. These measurements confirmed that, as the modulation is a low frequency digital modulation, results with HW devices and SW simulations match properly with differences smaller than 1 dB in the range in which the real HW is linear (avoiding HW saturation limit and equipment noise floor).

4.2. Channel Response Models under Test

Channel models are usually represented by its channel response function $H(f)$ defined in module and phase. For the tests described in this work, the following channels have been considered.

4.2.1. Flat Channel

This is the channel with the simplest response function. When this channel is applied, the received signal spectrum has the same amplitude and phase as the transmitted one for every frequency point.

4.2.2. Frequency Selective Channel

The proposed channel is a synthetic channel that was defined by the PRIME Alliance during the PRIME 1.4 PHY technology design process to test the performance of the system in a representative situation of a channel with a resonator in the center of the PRIME band. It is a filter of constant group delay: it introduces a distortion in amplitude depending on the frequency, but not in phase.

This filter was particularly designed to attenuate 10% of the carriers 20 dB or more in the center of the band. More precisely, the filter features a maximum attenuation at 62.5 kHz (considering a sampling frequency of 250 kHz). It has an attenuation of 20 dB for carriers between 60.4 and 64.5 kHz (9 carriers) and an attenuation of 40 dB for carrier between 61.8 and 63.1 kHz (3 carriers) and an attenuation higher than 60 dB to 1 single carrier. The frequency characterization of this filter is represented in Figure 3.

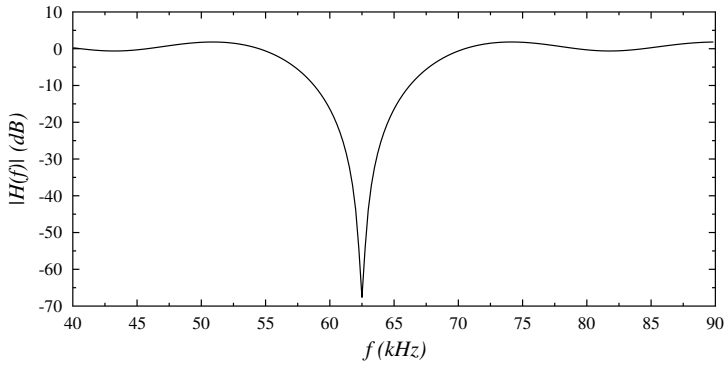

Figure 3. Frequency selective channel response module.

The frequency selective channel is defined by the impulse response $h[n]$ in Table 2. It is a Finite Impulse Response (FIR) filter of order 31. This impulse response in represented in Figure 4.

Table 2. Impulse response for a frequency selective channel.

n	*h[n]*	*n*	*h[n]*	*n*	*h[n]*	*n*	*h[n]*
0	-2.66375×10^{-5}	4	8.897×10^{-6}	8	-5.562×10^{-6}	12	2.36223×10^{-5}
1	0.0972533	5	0.0570675	9	0.072636	13	0.0814326
2	3.06855×10^{-5}	6	1.60698×10^{-5}	10	-3.19252×10^{-5}	14	-1.51506×10^{-5}
3	-0.0478325	7	-0.0654797	11	-0.0780915	15	1
Remaining values of $h[n]$ defined through symmetry: $h[n] = h[30 - n] \quad \forall n \in \mathbb{N}/16 \leq n \leq 30$							

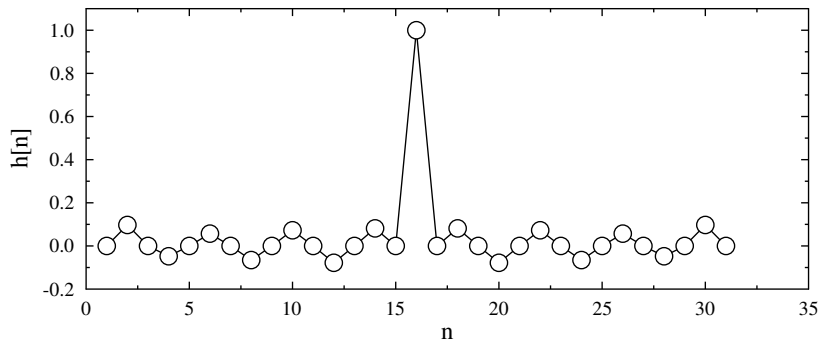

Figure 4. Impulse response of the frequency selective channel.

4.2.3. Abrupt Phase Shift Channel

Reference [6] shows several cases in which important phase shift conditions occur in real field situations. As modulation of each PRIME subcarrier is a phase differential modulation between carriers that are adjacent in frequency, analyzing how the standard behaves on a phase abrupt channel is particularly important.

This filter is specifically designed to have a π *rad* phase shift at 62.5 kHz (considering the nominal sampling frequency of 250 kHz). The phase of the frequency response is represented in Figure 5. It is a linear phase filter except for the abrupt phase change.

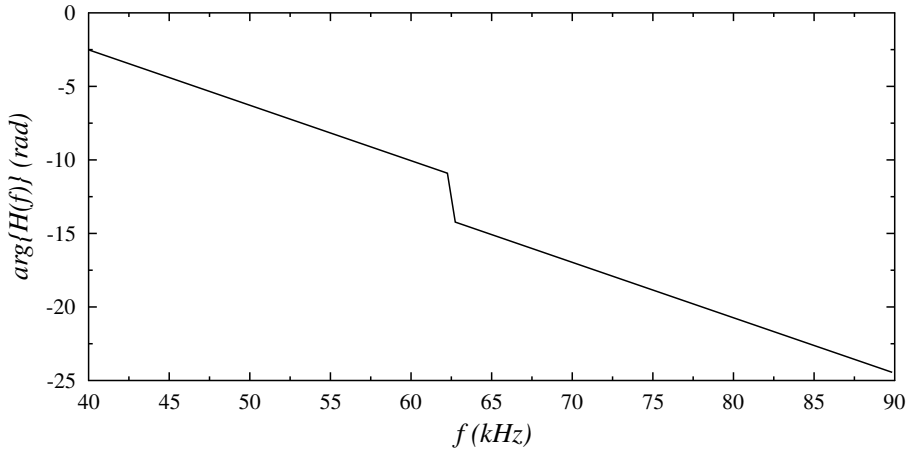

Figure 5. Frequency Response Phase of the abrupt phase change channel.

The filter also presents a small amplitude glitch in the phase shift point, which attenuates two carriers 20 dB and one single carrier 40 dB. Figure 6 represents the module of the filter response.

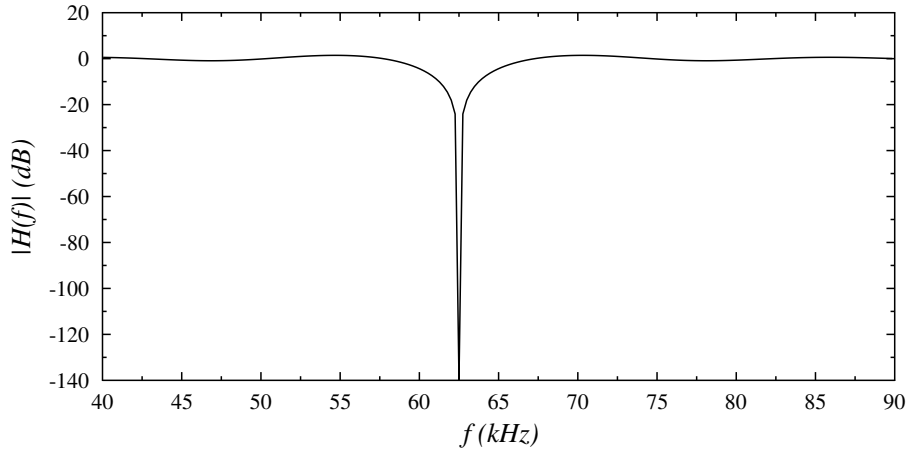

Figure 6. Module of the frequency response of abrupt phase change channel.

The channel with abrupt phase shift is defined by the impulsional response $h[n]$ shown in Table 3. It is a FIR filter of order 31. Figure 7 represents this impulsional response in time.

Table 3. Impulse response definition for abrupt phase shift channel.

n	*h[n]*	*n*	*h[n]*	*n*	*h[n]*	*n*	*h[n]*
0	−0.04244	4	−0.05787	8	−0.09095	12	−0.21221
1	0.00000	5	0.00000	9	0.00000	13	0.00000
2	0.04897	6	0.07074	10	0.12732	14	0.63662
3	−0.00000	7	−0.00000	11	−0.00000	15	0.00000
Remaining values of $h[n]$ defined through symmetry: $h[n] = h[30 - n] \quad \forall n \in \mathbb{N}/16 \leq n \leq 30$							

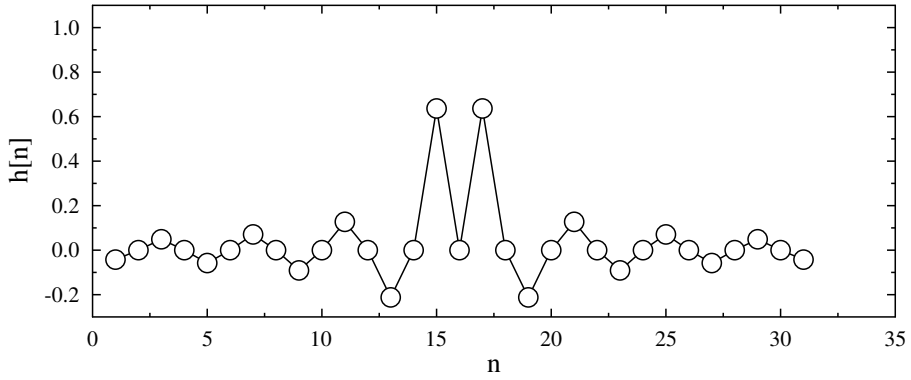

Figure 7. Impulse response of the abrupt phase shift channel.

4.3. Channel Noise Models under Test

4.3.1. Additive White Gaussian Noise (AWGN) Generation

AWGN is a representative synthetic example of the PLC background noise as defined in references like [2,3]. The AWGN generation has been performed in fixed point arithmetic, using the central theorem limit. For this purpose, the Gaussian variable is generated by adding 12 values of uniform distribution.

The uniform noise generator and the AWGN generator passed the Kolmogorov-Smirnoff test. The Kolmogorov-Smirnoff test with 1 million random values generated has a certainty higher than 99.9% to match the required distributions.

4.3.2. Synchronous Impulsive Noise

References like [1–3] describe the synchronous impulsive noise as being common in the PLC propagation channel. Since the frequency distribution of the synchronous impulsive noise is very variable, white synchronous impulsive noise has been selected for a direct comparison with respect to the background AWGN noise. Regarding the time distribution of the noise, the impulsive noise generation is carried out by modulating the amplitude of the AWGN noise with periodic square pulses, obtaining white periodic impulsive noise synchronous to the electric network, as traditionally classified in [1,2].

The following parameters are configurable:

- Pulse to Base Ratio (PBR). The ratio between the pulse power (P_{pulse}) and the base power (P_{base}) of the impulsive noise, configured in dB.
- Period (T). The period between pulses can be configured in μs.
- Duration (d). The duration of each pulse can be configured in μs.

Figure 8 describes every configurable parameter in a graph that represents noise power in time.

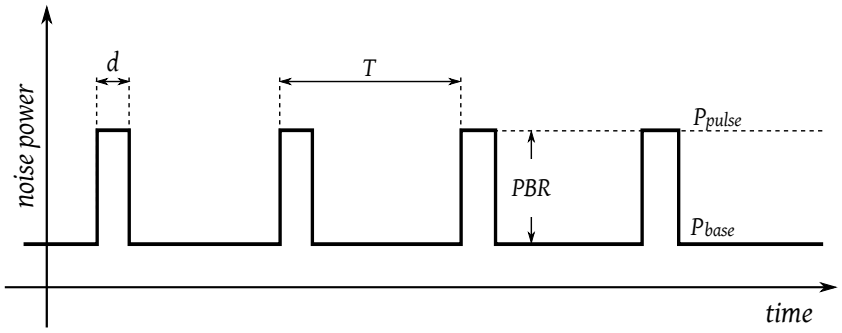

Figure 8. Synchronous impulsive noise power in time.

Integrating the described noise in time, the average power of the described noise (P_{noise}) is calculated in Equation (1).

$$P_{noise} = \frac{P_{base}\,(T-d) + P_{pulse}d}{T} = P_{base}\left(1 - \frac{d}{T}\right) + P_{pulse}\frac{d}{T} \tag{1}$$

Equation (1) can be extended to obtain the relation of P_{pulse} and P_{base} with P_{noise} after the configurable parameters PBR, d and T. These results are represented in Equations (2) and (3).

$$\frac{P_{pulse}}{P_{noise}} = 1 + PBR\left(1 - \frac{d}{T}\right) \tag{2}$$

$$\frac{P_{base}}{P_{noise}} = \frac{1}{PBR} + 1 - \frac{d}{T} \tag{3}$$

The synchronous impulsive noise PBR is fixed to 20 dB, whereas the period between pulses T is fixed to 10^4 μs. These parameters correspond to a 50 Hz network with powerful white periodic impulsive noise in both zero crossings, based on the experience of field deployments of ZIV devices. The duration of the pulse d remains variable.

4.4. Precision of the Simulations

4.4.1. FER Precision and Number of PPDUs

As a general rule, the quality control metric for each test is the FER. The FER has been selected instead of the Bit Error Rate (BER), due to the fact that many PHY procedures are performed once per PPDU, like frame alignment, equalization, header decoding and Viterbi decoder flushing. Additionally the impact in the Medium Access Control (MAC) is directly related to the FER as a frame error will discard completely a MAC packet independently of the number of erroneous bits. In order to understand the results, it is important to analyze the user perception regarding FER values.

- $FER = 10^{-1}$. This FER value is considered the minimum acceptable value so communication can be started. Although many losses are expected, communication is feasible in this environment. Since it is a minimum value, it is unlikely that at Medium Access Control (MAC) level one device with this PPDUs loss rate could become a repeater for others and keep a stable topology. Some narrowband PLC technologies make their sensitivity limit for $FER = 10^{-1}$, such as [20].
- $FER = 5 \times 10^{-2}$. This FER value is used for some narrowband technologies as the quality threshold for good communication. Reference [21] considers this threshold for PLC communication without errors (considering that this percentage of errors will be solved by higher layers).

- $FER = 10^{-2}$. This more restrictive FER value is considered a satisfactory FER for the performance of this technology. One device operating with this amount of FER can behave thoroughly as a repeater. The PRIME Alliance uses this value as its threshold in reference [22].

For better FER values (such as FER of 10^{-3}), performance is exceptionally good and the probability of losing a PPDU will not be the limiting factor. It can be considered that in these scenarios there will be other limiting factors, such as MAC collisions, time or spatial variability, *etc*.

Obtaining low FER values with precision through simulation requires a high number of simulated PPDUs (and long simulation periods).

The number of PPDUs required to obtain precise FER values were determined by calculating normalized standard deviation of the estimated FER, this is, the standard deviation of the estimated FER ($\sigma(FER')$) compared to the real FER. Results of these calculations are summarized in Figure 9.

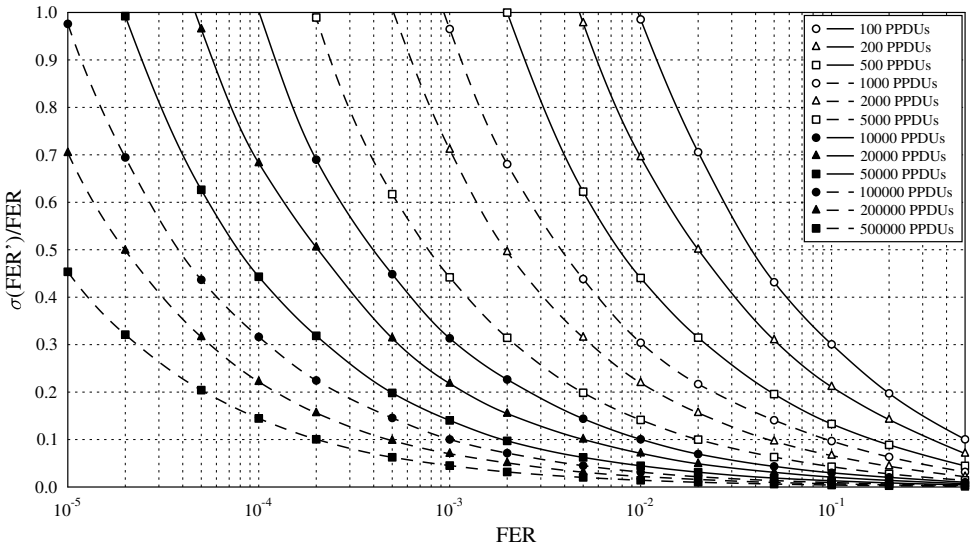

Figure 9. Relation $\sigma(FER')/FER - FER$.

Considering the above criteria, and it being the case that $FER = 10^{-3}$ is of exceptionally good quality, the precision limit is considered to be sufficient when the probability of being better than $FER = 2 \times 10^{-3}$ is higher than 99.9% (still five times better than $FER = 10^{-2}$). This happens for $\sigma(FER')/FER$ lower than 0.32. Figure 9 shows that simulations with 10,000 PPDUs are precise enough.

4.4.2. SNR Precision and SNR Range for Each Test

For SNR computation, only the noise in band is considered, this is, the noise power within the bandwidth assigned to PRIME transmissions. The precision in the generated SNR magnitude is lower than 0.01 dB.

The SNR increment for each test point is 0.1 dB. It has to be small enough as these digital communications tend to have great variations in 1 or 2 dB.

The SNR range for each test has been experimentally estimated by performing a fast simulation of 100 or 1000 PPDUs every 1 dB of SNR in a very wide SNR range. Based on this estimation, the useful SNR range for the final simulation was selected.

4.4.3. Tests Execution

The tests have been designed to be executed automatically in an unattended batch process.

The simulation of every point has required the transmission and reception of 26,110,000 PPDUs, or the equivalent time of 104 hours of simulated network. This high computational time is the result of complying with the FER and SNR precision requirements defined in the previous subsections.

5. Methodology

The study of the influence of the channel distortions on ITU-T G.9904 (PRIME) technology is based on simulations of the described PHY layer. Different transmission and channel parameters are analyzed in order to relate these parameters with the resulting FER.

The simulation tool is able to configure a physical transmitter and receiver and modify the parameters of the communication and channel effects, and then evaluate the communication quality by measuring the resulting FER.

5.1. Channel Simulation Environment with Full Transmitter-Receiver

This section is focused on the simulations of the PHY layer of the full transmitter-receiver chain of PRIME version 1.3.6.

The transmission and reception tests of the PHY layer are composed of the following three blocks: the transmitter block, the propagation channel model and the receiver block. The transmitter block contains the complete PHY layer as in Figure 1, and it is in charge of generating the PRIME 1.3.6 standard signal with some configurable parameters. The propagation channel model is different depending on the test to perform. The receiver is a complete PRIME 1.3.6 receiver as described in Figure 2, which tries to decode the signal distorted by the channel simulator in order to measure the FER.

5.2. Configurations under Test

Several tests have been designed and performed to evaluate different aspects of the communication stack and the dependency with the channel parameters.

- AWGN channel test. It is a test of the whole transmission and reception chain with a flat channel and AWGN noise. It is the base reference test, used as a reference for the rest of the performed tests, to relate how changes in the different parameters affect the system behavior. Results are described in Section 6.1.
- Synchronous impulsive Noise channel test. The test inserts in the propagation channel synchronous impulsive noise of variable duration. This test aims at evaluating the robustness of the system to synchronous impulsive noises of different temporal distribution of the noise power. Results are described in Section 6.2.
- Selective channel test. The purpose of this test is to check the robustness of the communications in the presence of an important attenuation on some of the subcarriers. Results are described in Section 6.3.
- Abrupt Phase channel test. For this particular channel, the distortion to be tested is an abrupt phase shift of π *rad* in the center of the band. Results are described in Section 6.4.

Table 4 summarizes the detailed information of the configuration for each test whose results are detailed in Section 6.

Table 4. Test configurations studied.

Test Configuration	Channel Response	Noise Model	Subcarrier Modulation	PSDU Length
Channel simulation TX-RX				
- AWGN	Flat	AWGN	All	256 bytes
- Impulsive Noise	Flat	Impulsive	$DBPSK_F$	256 bytes
- Selective Channel	Selective	AWGN	$DBSPK_F$–$D8PSK_F$	256 bytes
- Abrupt Phase Channel	Abrupt Phase	AWGN	$DBSPK_F$–$D8PSK_F$	256 bytes

6. Results

The following figures relate FER and SNR values for different channel parameter values and/or modulation schemes.

6.1. AWGN

Figure 10 shows the relation between SNR and FER for each modulation scheme, with and without the convolutional encoding (solid and dashed lines respectively).

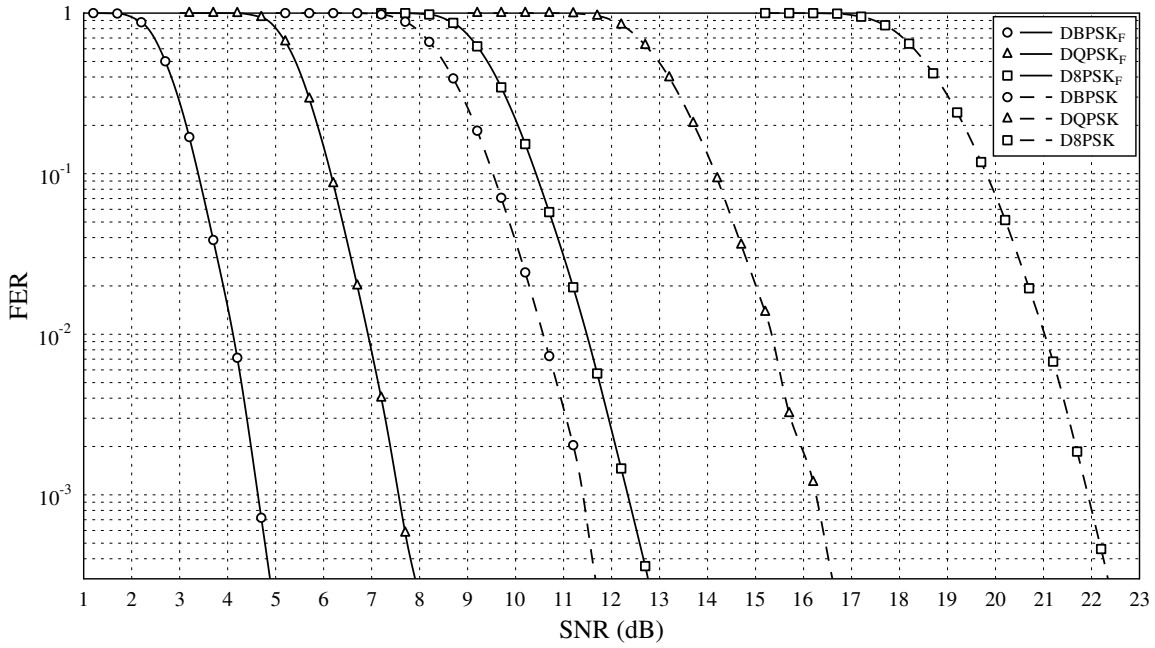

Figure 10. Relation FER-SNR for AWGN flat channel with payload of 256 bytes.

Transition of FER values from 10^{-1} to 10^{-2} happens in just 0.8 dB for coding systems with convolutional encoder, while it is approximately 1 or 1.2 dB for schemes without the convolutional encoder.

As expected, results demonstrate the influence of the convolutional encoding on the robustness of the received signal. Sensitivity differences of 6.5 dB for DBPSK, 8.5 dB for DQPSK and 9.5 dB for D8PSK have been obtained in the tests.

When the convolutional encoder is used, the difference between DBPSK and DQPSK is approximately 3 dB of SNR in order to obtain the same FER value, whereas for D8PSK, sensitivity is 4.5 dB below DQPSK.

The rate of the convolutional encoder is 1/2. The lengths of the PPDUs without convolutional encoders are approximately the half of the ones with convolutional encoder, decreasing the transmitted energy for each PPDU by approximately 3 dB. Not using the convolutional encoding has a saving in energy of 3 dB, but a consequence in the reception sensitivity of 6.5 dB, 8.5 dB and 9.5 dB (for DBPSK, DQPSK and D8PSK respectively). This situation makes the modes without convolutional encoding have much worse performance for the same input energy, making them not usable in practice, considering that a certified PRIME product has to be capable of using both. This result is in line with the conclusions obtained in [23].

Figure 10 shows that DBPSK mode without convolutional encoding is particularly useless as the usable rate is similar to the DQPSK with convolutional encoding but with reduced robustness.

6.2. Synchronous Impulsive Noise

This test is performed according to Section 5.1 with a flat response propagation channel with additional synchronous impulsive noise as described in Section 4.3.2.

SNR value is the ratio of signal power (P_{signal}) to noise average power (P_{noise}). As described in Equation (1), the noise average power (P_{noise}) is calculated by weighting the base noise power (P_{base}) and the (P_{pulse}) through the total length of the noise. Equations (2) and (3) confirm that the pulse power and base power of the impulsive noise depend on the duration of the pulses. The aim of this test is to compare the impact of different temporal distributions of the same average noise power.

Figure 11 shows the relation between SNR and FER as a function of the impulsive noise duration for DBPSK with convolutional encoder.

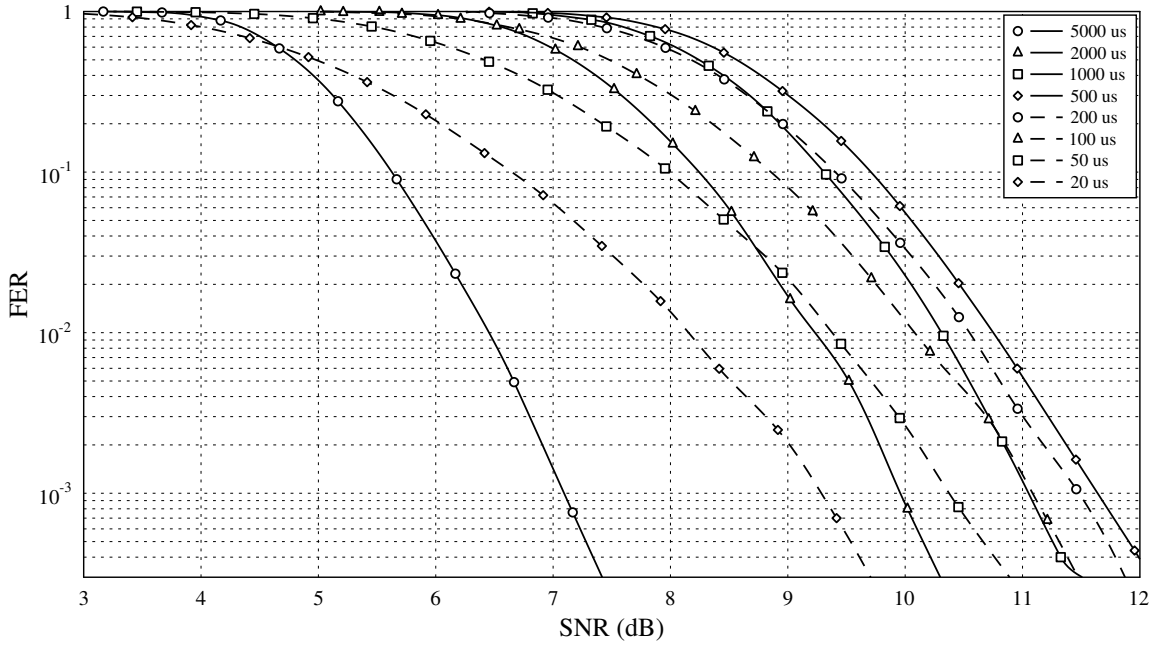

Figure 11. Relation FER-SNR affected by synchronous impulsive noise with different duration.

Results for synchronous impulsive noise scenario have a turning point when the noise duration is of 500 μs.

For pulses of noise of a duration under 500 μs, the shorter the pulse, the lower the FER for the same SNR (or the lower the SNR for the same FER). In these cases, the noise is considered impulsive as it is much shorter than a symbol, and the gain for impulsive noise of the OFDM technology is obtained.

On the contrary, in Figure 11, for pulses of duration higher than 500 μs, the longer the pulse, the lower the FER for the same SNR. In this situation, the duration of the pulse begins to be comparable with the length of one OFDM symbol 2240 μs. The duration of the pulses may be high enough to corrupt a complete OFDM symbol and the interleaver (block interleaver of one OFDM symbol) will not avoid introducing a burst error to the Viterbi decoder, making the frame unrecoverable. Considering this, the duration is high enough to make the coding gain not useful and the pulse power (P_{pulse}) will be the limiting factor. Equation (2) demonstrates that synchronous impulsive noise with longer pulses (higher d) have lower pulse power (P_{power}) for the same SNR (same P_{signal} and P_{noise}). As the same energy is widespread in time, the probability of corrupting a whole OFDM symbol is reduced and, consequently, the FER.

Additionally, comparing the results for 500 μs in Figure 11 with the results of $DBPSK_F$ in Figure 10, it can be concluded that variations in amplitude of the noise of 20 dB in the form of impulsive noise affect to PRIME sensitivity up to 7.75 dB.

6.3. Frequency Selective Channel

Physical layer tests for a frequency selective channel scenario are described in Section 5.1 applying AWGN noise and the channel described in Section 4.2.2.

This test is considered for modulation schemes with convolutional encoding only, as frequency selective channels remove some of the subcarriers making every modulation scheme without error correction unsuccessful.

Figure 12 represents the relation between FER and SNR values for each modulation schemes with convolutional encoding.

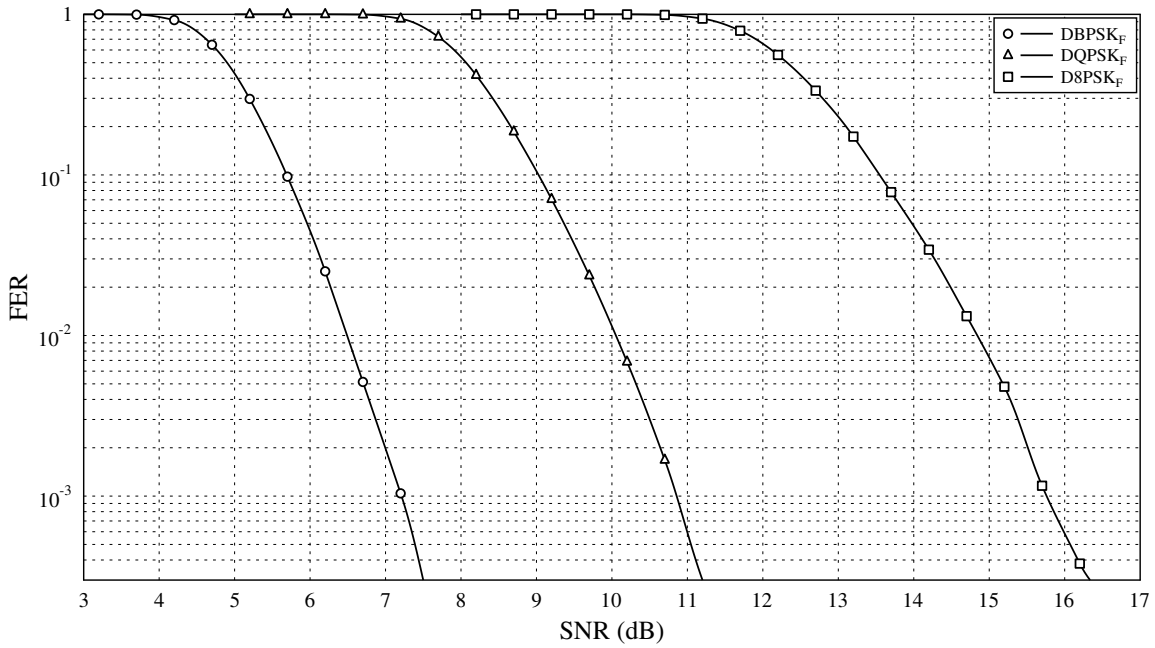

Figure 12. Relation FER-SNR with frequency selective channel.

This graph shows how for frequency selective channel scenarios, using DBPSK with convolutional encoder, a SNR of 6.5 dB is required for $FER\ 10^{-2}$. For DQPSK with convolutional encoder, a SNR of 10 dB is required (3.5 dB more than DBPSK), and for D8PSK with convolutional encoder, a SNR of 14.8 dB (8.3 dB more than DBPSK).

Comparing the results in Figure 12 and the results obtained with a flat channel in Figure 10, the sensitivity loss due to the selective channel can be measured. The sensitivity loss compared to a flat channel is of 2.5 dB for DBPSK, 3 dB for DQPSK and 3.5 dB for D8PSK.

6.4. Channel with Abrupt Phase Shift

Tests are executed according to the method described in Section 5.1 with the particular propagation channel described in Section 4.2.3.

Given the fact that this type of propagation channel invalidates the subcarrier (or subcarriers) of the abrupt phase shift moment, error correction mechanisms are essential when this type of channel distortions occur. Therefore, only modulation schemes with convolutional encoding are analyzed.

Figure 13 relates FER and SNR values for each modulation scheme with convolutional encoding.

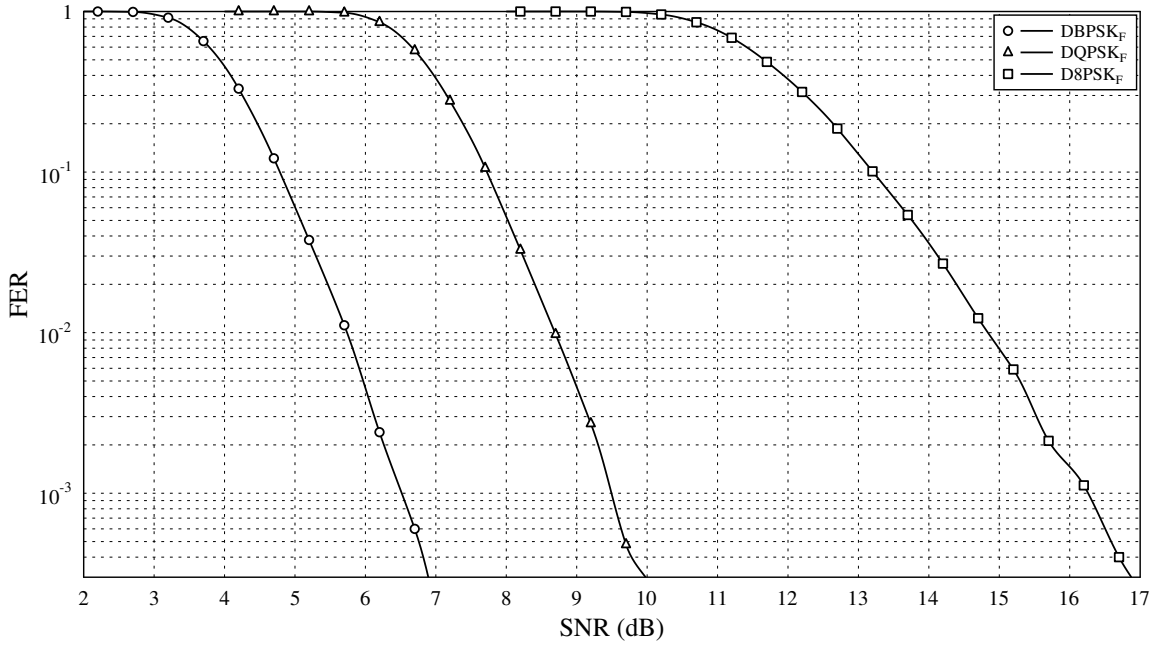

Figure 13. Relation FER-SNR with abrupt phase shift channel.

The SNR necessary for communications with an FER value of 10^{-2} is 5.75 dB for DBPSK with the convolutional encoder, 8.75 dB for DQPSK with the convolutional encoder (3 dB higher than DBPSK), and 14.75 dB for D8PSK with the convolutional encoder (around 9 dB higher than DBPSK).

To obtain conclusions on how this abrupt phase channel impacts PRIME technology, the results presented in Figure 13 are compared to the flat channel results in Figure 10. The abrupt phase shift introduces a sensitivity loss of approximately 1.75 dB for DBPSK and DQPSK with convolutional encoding. For D8PSK with convolutional encoding, the penalty obtained in the tests is 3.25 dB.

7. Conclusions

Based on the results obtained in Section 6, different conclusions may be obtained:

- Regarding the usability of the PHY modes without convolutional coding, the results show that the transmission modes without convolutional encoding are not valid for practical use. The consequences of not using convolutional encoding are particularly severe in situations of impulsive or frequency selective channels, as the channel erases or distorts one of the carriers, and it is not possible to decode any PPDU without any kind of error correction.
- PRIME standard shows high robustness against tough channel conditions (frequency selective channel or channel with abrupt phase change), being the decoding sensitivity usually impacted by less than 3 dB.
- The presence of synchronous impulsive noise and its duration or waveform are very important for analyzing the PRIME communications sensitivity.

These conclusions lead to a better understanding of the PRIME standard behavior to individual channel effects. First, the obtained results can be used as reference values in field deployment once the main effects of these deployments are identified. Second, the understanding of the results also open the door to future improvements in designing and development of equipment.

Acknowledgments: This work has been partially supported by the Spanish Ministry of Economy and Competitiveness (project TEC2015-67868-C3-1-R), the Basque Government (project IT 683-13) and the University of the Basque Country (UPV/EHU) within the program for the specialization of the postdoctoral researcher staff.

Author Contributions: Asier Llano has developed the simulation tool, defined the analysis methodology, run the tests and analyzed the results; Itziar Angulo has contributed in the definition of channel models and in the analysis of the results; Txetxu Arzuaga has validated the workbench according to PRIME standard; Pablo Angueira and David de la Vega have led the research work.

Conflicts of Interest: The authors declare no conflict of interest. Similar PLC studies to this one are being carried by some of the authors of this article using other PLC technologies, such as ITU-T G.9903 (G3-PLC) and IEC 61334 (SFSK). Other technologies like ITU-T G.9902 (G.hnem) will be considered for future PLC studies.

References

1. O'Neal, J.B., Jr. The residential power circuit as a communication medium. *IEEE Trans. Consum. Electron.* **1986**, *32*, 567–677.
2. Hooijen, O.G. A channel model for the low-voltage power-line channel; Measurement and simulation results. In Proceedings of the IEEE International Symposium on Powerline Communications, Essen, Germany, 2–4 April 1997; pp. 51–56.
3. Hooijen, O.G. A channel model for the residential power circuit used as a digital communications medium. *IEEE Trans. Electromagn. Compat.* **1998**, *40*, 331–336.
4. Tlich, M.; Chaouche, H.; Zeddam, A.; Pagani, P. Novel approach for PLC impulsive noise modelling. In Proceedings of the IEEE International Symposium on Powerline Communications, Dresden, Germany, 29 March–1 April 2009; pp. 20–25.
5. Gassara, H.; Rouissi, F.; Ghazel, A. Narrowband stationary noise characterization and modelling for power line communication. In Proceedings of the IEEE International Symposium on Powerline Communications, Surat Thani, Thailand, 4–6 September 2013 ; pp. 148–153.
6. Wenqing, L.; Sigle, M.; Dostert, K. Channel phase distortion and its influence on PLC systems. In Proceedings of the IEEE International Symposium on Powerline Communications, Beijing, China, 27–30 March 2012; pp. 268–273.
7. Mitra, J.; Lampe, L. Coded narrowband transmission over noisy powerline channels. In Proceedings of the IEEE International Symposium on Powerline Communications, Dresden, Germany, 29 March–1 April 2009; pp. 143–148.
8. Ndo, G.; Siohan, P.; Hamon, M.H. OFDM/OQAM performance analysis under asynchronous impulsive noise. In Proceedings of the IEEE International Symposium on Powerline Communications, Dresden, Germany, 29 March–1 April 2009; pp. 160–165.
9. Matanza, J.; Alexandres, S.; Rodriguez-Morcillo, C. PRIME performance under impulsive noise environments. In Proceedings of the IEEE International Symposium on Powerline Communications, Beijing, China, 27–30 March 2012, pp. 380–385.
10. Kim, I.H.; Varadarajan, B.; Dabak, A. Performance analysis and enhancements of narrowband OFDM powerline communication systems. In Proceedings of the IEEE International Conference on Smart Grid Communications, Gaithersburg, MD, USA, 4–6 October 2010; pp. 362–367.
11. Hoch, M. Comparison of PLC G3 and PRIME. In Proceedings of the IEEE International Symposium on Power Line Communications and Its Applications, Udine, Italy, 3–6 April 2011; pp. 165–169.
12. Meyer, J.; Bollen, M.; Amaris, H.; Blanco, A.M.; Gil de Castro, A.; Desmet, J.; Klatt, M.; Kocewiak, Ł.; Rönnberg, S.; Yang, K. Future work on harmonics—Some expert opinions Part II—Supraharmonics, standards and measurements. In Proceedings of the IEEE International Conference on Harmonics and Quality of Power, Bucharest, Romania, 25–28 May 2014; pp. 909–913.
13. Bollen, M.; Olofsson, M.; Larsson, A.; Ronnberg, S.; Lundmark, M. Standards for supraharmonics (2 to 150 kHz). *IEEE Electromagn. Compat. Mag.* **2014**, *3*, 114–119
14. CENELEC SC 205A. *Mains Communicating Systems TF EMI Study Report on Electromagnetic Interference Between Electrical Equipment/systems in the Frequency Range below 150 kHz*, 2nd ed.; European Committee for Electrotechnical Standardization (CENELEC): Brussels, Belgium, 2013.
15. *G.9904 Narrowband Orthogonal Frequency Division Multiplexing Power Line Communication Transceivers for PRIME Networks*; Telecommunication Standardization Sector (ITU-T) of the International Telecommunication Union (ITU): Geneva, Switzerland, 2012.
16. *G.9901 Narrowband Orthogonal Frequency Division Multiplexing Power Line Communication Transceivers—Power Spectral Density Specification*; ITU-T: Geneva, Switzerland, 2012.

17. PRIME Technical Working Group. *Specification for PoweRline Intelligent Metering Evolution 1.3.6.*; Prime Alliance: Brussels, Belgium, 2012.
18. ZIV Metering Solutions Home Page. Available online: http://www.meteringsolutions.ziv.es (accessed on 5 October 2015).
19. PRIME Certification Working Group. *PRIME Certification Test Cases, Version 1.2*; Prime Alliance: Brussels, Belgium, 2010.
20. *IEEE Standard 1901.2-2013—IEEE Standard for Low-Frequency (less than 500 kHz) Narrowband Power Line Communications for Smart Grid Applications.*; IEEE: Piscataway, NJ, USA, 2013.
21. *Performance Assessment of G3-PLC for Smart Grid Applications. Ref:3002002917*; Electric Power Research Institute (EPRI): Palo Alto, CA, USA, 2014.
22. PRIME Alliance Technical Working Group. *PRIME v1.4 White Paper*; PRIME Alliance: Brussels, Belgium, 2014.
23. Sendín, A.; Llano, A; Angueria, P. Análisis de la utilización efectiva de los esquemas de modulación de la especificación PRIME para la lectura remota de contadores. In Proceedings of the XIX Telecom I+D, Madrid, Spain, 24 November 2009. (In Spanish)